

# EXPERIMENTAL CHARACTERIZATION OF INJECTION PROBES FOR BULK CURRENT INJECTION

**S. A. Pignari<sup>(1)</sup>, F. Grassi<sup>(2)</sup>, F. Marliani<sup>(3)</sup>, F. G. Canavero<sup>(4)</sup>**

<sup>(1)</sup> *Politecnico di Milano, Dipartimento di Elettrotecnica - P.za Leonardo da Vinci, 32, I-20133, Italy,  
Email: [sergio.pignari@polimi.it](mailto:sergio.pignari@polimi.it)*

<sup>(2)</sup> *As (1) above, but Email: [flavia.grassi@polimi.it](mailto:flavia.grassi@polimi.it)*

<sup>(3)</sup> *Electromagnetics and Space Environment Division, European Space Agency - Keplerlaan 1, NL-2201, Noordwijk,  
The Netherlands, Email: [filippo.marliani@esa.int](mailto:filippo.marliani@esa.int)*

<sup>(4)</sup> *Politecnico di Torino, Dipartimento di Elettronica – C.so Duca degli Abruzzi, 24, I-10129, Italy,  
Email: [flavio.canavero@polito.it](mailto:flavio.canavero@polito.it)*

## ABSTRACT

In this work, a lumped-parameter circuit model of injection probes for bulk current injection (BCI) is derived from probe input-impedance measurement. The model accounts for the effects related to ferrite magnetic-core losses and degradation of the magnetic permeability with frequency. Model assessment is achieved by comparing predictions of currents induced by BCI in the terminations of an electrically-long single-ended interconnection with direct measurements in a real BCI test applied to the same structure. The proposed model provides a precise description of the coupling between the probe and the wiring under test for frequencies up to 500 MHz.

## INTRODUCTION

The assessment of bulk current injection (BCI) versus other conducted susceptibility tests requires precise modeling of injection probes in a bandwidth extending up to hundreds of MHz. This implies the need to improve the canonical model developed in [1], where a low-frequency, lossless, inductive model of the injection probe was developed.

In this paper, this problem is addressed by treating the probe as radio-frequency (RF) transformer with both the primary and the secondary windings acting as distributed-parameter magnetically coupled structures. An approximated, three-port lumped-parameter model of the probe is derived, which exploits experimental data of the probe input impedance (measured via a network analyzer (NA) in terms of reflection coefficient). This approach allows for the inclusion into the probe model of the frequency response of the ferrite core, i.e., the effects related to the degradation of the magnetic permeability of the ferrite core with frequency, as well as the core losses.

Predictions obtained by the proposed model are assessed by analyzing a simple BCI setup, composed of a commercially available injection probe clamped on a single-ended wiring with known terminal loads. Comparison of the voltage levels actually induced by BCI in the wiring loads (obtained by measurement) with predictions based on the use of the proposed probe model indicates an appreciable agreement up to 500 MHz.

## LUMPED-PARAMETER CIRCUIT MODEL OF THE INJECTION PROBE

The lumped-parameter circuit used to model the injection probe is sketched in Fig. 1(a). In the circuit, the radio-frequency (RF) source feeding the probe is represented by a Thevenin equivalent circuit with open-end voltage source  $V_{RF}$ , and internal impedance  $R_S = 50\Omega$ . The probe model is based on a low-frequency transmission line (TL) interpretation of the two magnetically coupled coils (i.e., the primary winding and the wiring clamped by the probe). Accordingly, lumped equivalent-circuits are used to model the windings and the input connector/adaptor of the probe. In particular,  $C_1$  and  $L_{1w0}$  account for capacitive and inductive coupling between the primary winding and the inner surface of the metallic body of the probe;  $C_2$  describes capacitive coupling between the metallic body of the probe and the clamped conductor;  $C_C$  and  $L_C$  are used to model the chain connection of the SMA-to-N adaptor and the N connector mounted at the input port of the probe. The inductance  $L_C$  affects the probe behavior for frequencies above 400 MHz. Conversely, the capacitance  $C_C$  typically prevails over  $C_1$  and its contribution to the frequency response of the probe extends at lower frequencies. Estimates for these parameters are provided in [2]. The frequency behavior of the ferrite core is accounted in the model of Fig. 1(a) by the complex and frequency-dependent coupled inductances  $\hat{L}_1(\omega)$ ,  $\hat{L}_2(\omega)$ . The probe frequency response is deeply influenced by these parameters, whose frequency dependence is due to magnetic dispersion and core losses.

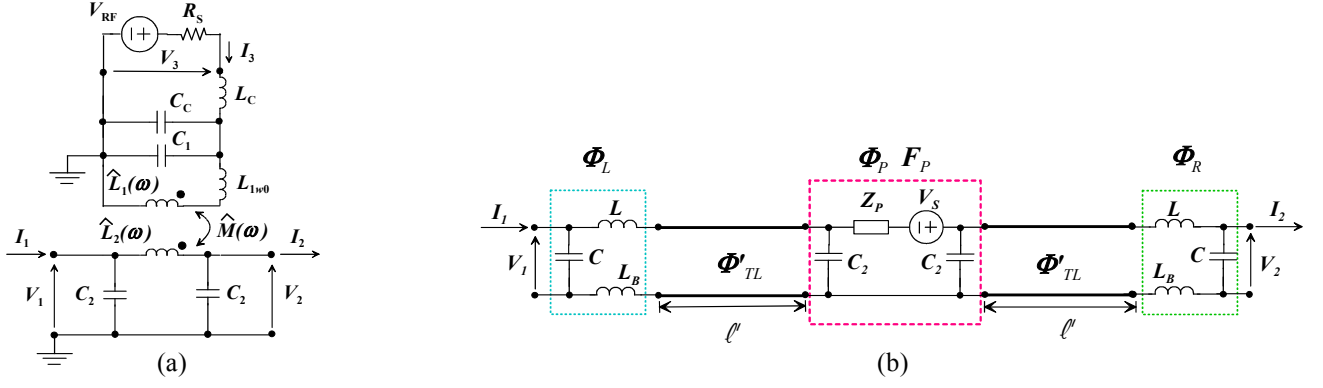


Fig. 1. (a) Lumped-parameter circuit model of the injection probe fed by an RF generator. (b) Chain parameter representation of the BCI setup with the probe mounted at the midpoint of the test conductor.

An estimate for the self inductance  $\hat{L}_1(\omega)$  is obtained by measuring the reflection coefficient  $S_{33}$  at the probe input (in absence of the secondary circuit) and by comparing this quantity with the analytical expression of  $S_{33}$ , evaluated from the model in Fig. 1(a) as a function of the circuit parameters [2]. This operation leads to the following expression of the self-inductance  $\hat{L}_1(\omega)$ :

$$\hat{L}_1(\omega) = \frac{R_0(1+S_{33})/(1-S_{33}) - j\omega L_C}{j\omega\{j\omega(C_C + C_1)[j\omega L_C - R_0(1+S_{33})/(1-S_{33})] + 1\}} - L_{1w0} \quad (1)$$

where  $R_0 = 50\Omega$  is the reference resistance used to define the scattering parameters. Consequently, the frequency response of the ferrite core results to be fully described by the complex and frequency-dependent reluctance  $\hat{\mathfrak{X}}(\omega) = N_1^2 / \hat{L}_1(\omega)$ , where  $N_1$  denotes the number of turns of the primary winding. The self-inductance  $\hat{L}_2(\omega)$  and the mutual inductance  $\hat{M}(\omega)$  take the following expressions:

$$\hat{M}(\omega) = N_1 / \hat{\mathfrak{X}}(\omega); \quad \hat{L}_2(\omega) = 1 / \hat{\mathfrak{X}}(\omega) + L_{2d}, \quad (2)$$

where  $L_{2d}$  is the leakage inductance associated with the secondary winding. An estimate for this parameter is obtained by evaluating the flux confined between the secondary winding (i.e., the clamped conductor) and the inner surface of the probe core.

## REAL VERSUS VIRTUAL BCI TESTS

In order to assess the effectiveness of the probe model described in the previous section, predictions of the voltages induced via BCI in the terminal loads of a single-ended interconnection (virtual BCI test) are compared versus experimental data of the same voltages measured on a real BCI setup (real BCI test). This setup is composed of a bare wire (the conductor clamped by the probe) running parallel to a metallic ground plane, and connected via pass-through SMA connectors and vertical metallic strips to suitable terminal loads. The geometrical dimensions of the setup are: (a) wire radius  $r_w = 0.4\text{mm}$ ; (b) wire height above ground  $h = 5.1\text{cm}$ ; (c) wire length  $\ell = 66\text{cm}$ .

This structure, even if simple, is intended to reproduce the main coupling and propagation phenomena involved in a real BCI test, where the injection probe clamps a wiring harness connecting the equipment under test (EUT) to auxiliary equipment (AE).

### Real BCI Test

Scattering parameters measurements were carried out with an injection probe (FCC F-130A, [3]) mounted at the midpoint of the above-described BCI setup. In the test, the input port of the probe (port no. 3) was connected to the transmitting port of the NA (Agilent E5070B). The receiving port of the NA was connected to one of the two terminations of the single-ended wiring (port no. 2), the other (port no. 1) being attached to a known load (the following impedance values

were used for this load:  $Z_L = 50\Omega$  and  $Z_L = \infty$ ). Accordingly, the transfer ratio  $V_2/V_{RF}$  between the voltage measured across port no. 2 (setup termination) and the open-end RF voltage source applied at port no. 3 (injection probe) is related to the scattering parameter  $S_{23}$  by the relationship:

$$V_2/V_{RF} = S_{23}/2 \quad (3)$$

Measurement data of the magnitude and phase of the voltage transfer ratio in (3) are reported in Fig. 2 (dotted curves).

### Virtual BCI Test

Virtual BCI testing is aimed at reconstructing the transfer ratio in (3) by resorting to the lumped-parameter model of the injection probe in Fig. 1(a). In order to obtain an analytical expression for such a transfer function, the whole BCI setup is modeled as the cascade connection of five blocks, as sketched in Fig. 1(b). In this figure, the injection probe fed by the NA transmitting port is modeled via the lumped-parameter circuit in Fig. 1(a). In Fig. 1(b), the parameters  $V_S$ ,  $Z_P$  represent the open-end voltage source and the series impedance of the Thevenin equivalent of the primary circuit as seen by the clamped wiring. In terms of chain parameters, the central block in Fig. 1(b) is described by matrix  $\Phi_P$  (representing the loading effect that the probe acts on the wiring under test) and vector  $F_P$  (describing the ability of the probe to inject energy onto the clamped wiring).

The other blocks in Fig. 1(b) describe the effects related to the BCI setup. In particular, the two line-sections in which the wiring is divided due to the presence of the probe are modeled by ideal TLs running above a perfect ground plane. Accordingly,  $\Phi'_{TL}$  denotes the chain-parameter matrix of a TL with characteristic impedance  $Z_C \approx 330\Omega$ , propagation constant  $\gamma = j\omega/c_0$  ( $c_0$  being the speed of light in free-space), and length  $\ell' = (\ell - \ell_p)/2$ , where  $\ell_p$  is the probe thickness.

The terminal sections of the BCI setup are modeled by suitable lumped-parameter circuits, represented by matrices  $\Phi_L$  and  $\Phi_R$ . These blocks account for the transmission properties of the pass-through connectors and field transition effects. The inductance  $L_B$  represents the partial inductance of the vertical metallic strips. This parameter is estimated via the analytical model in [4]. Conversely, parameters  $L$  and  $C$  are evaluated from scattering parameters measurements at the output ports of the setup with the probe removed. For the setup under analysis, one obtains:  $L_B \approx 17\text{nH}$ ,  $L \approx 20\text{nH}$ ,  $C \approx 3.3\text{pF}$ . At the setup terminations, voltages and currents are related by:

$$\begin{pmatrix} V_2 \\ I_2 \end{pmatrix} = \Phi \cdot \begin{pmatrix} V_1 \\ I_1 \end{pmatrix} + F, \quad (4a)$$

$$V_1 = -Z_L I_1, \quad V_2 = R_0 I_2, \quad (4b)$$

where:

$$\Phi = \Phi_R \cdot \Phi'_{TL} \cdot \Phi_P \cdot \Phi'_{TL} \cdot \Phi_L = \begin{bmatrix} \Phi_{11} & \Phi_{12} \\ \Phi_{21} & \Phi_{11} \end{bmatrix}; \quad F = \Phi_R \cdot \Phi'_{TL} \cdot F_P = V_S \begin{pmatrix} A_1 \\ A_2 \end{pmatrix}, \quad (4c)$$

The voltage transfer ratio  $V_2/V_{RF}$  is readily obtained from (4a), (4b), and (4c) as:

$$\frac{V_2}{V_{RF}} = \frac{(\Phi_{21}Z_L - \Phi_{11})A_1 - (\Phi_{11}Z_L - \Phi_{12})A_2}{\Phi_{21}Z_LR_0 - \Phi_{11}(Z_L + R_0) + \Phi_{12}} R_0 H(\omega) \quad (5)$$

where the function  $H(\omega) = V_S/V_{RF}$  (here omitted for brevity) depends on the parameters of the primary circuit of the probe. Magnitude and phase of voltage transfer ratio in (5) are reported in Fig. 2 (solid and dashed curves). Solid curves (labeled as Prediction A) are predictions resorting to (5) and to the probe model in Fig. 1(b). Dashed curves (labeled as Prediction B) are obtained by neglecting the loading effect of the probe on the clamped conductor (i.e., by assuming  $Z_P = 0$  and  $C_2 = \infty$ ). This allows to evidence the role of the passive parameters of the probe on the injection test. Globally, predictions turn out to be appreciably close to measurement data for frequencies up to 500 MHz.

## CONCLUSION

In this work, a lumped-parameter circuit model of injection probes employed in BCI tests has been developed and assessed. The proposed model is based on a preliminary experimental characterization of the injection probe (in terms of input impedance), and describes effects that are peculiar for effective prediction of the injection characteristics of the probe in the hundred of MHz range. Model effectiveness has been tested on a simple real BCI setup. Comparison of predictions versus experimental data indicates that this model is suited to explain the injection probe behavior for frequencies up to 500 MHz.

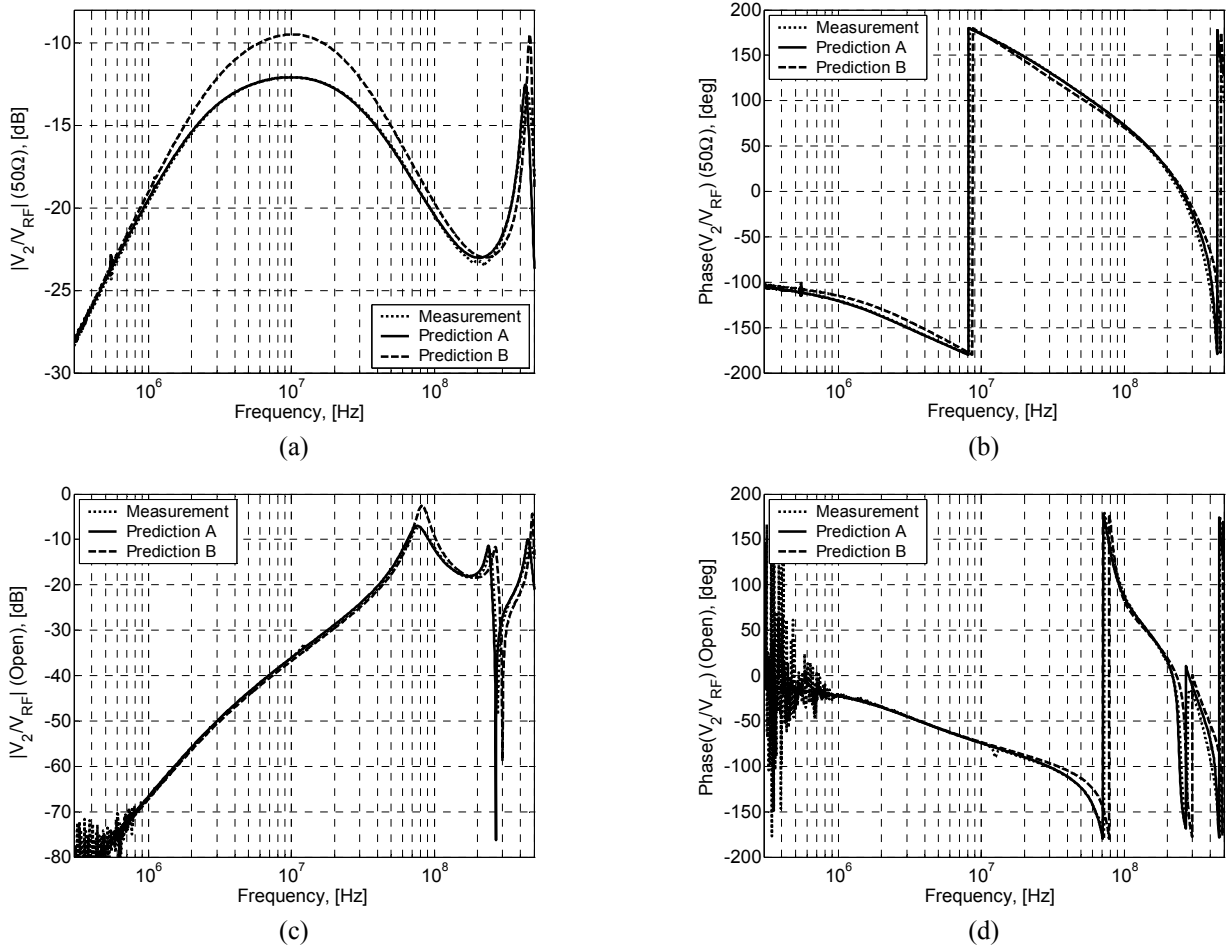


Fig. 2. Magnitude (a), (c) and phase (b), (d) of the transfer ratio between the voltage across one of the terminal loads of the BCI setup and the RF source  $V_{RF}$  feeding the injection probe. The dotted curves were obtained by measurement (via an NA); the solid and dashed curves represent predictions based on the proposed model (see text for details). Plots in (a), (b) are obtained with  $Z_L = 50\Omega$ . Plots in (c), (d) are obtained with  $Z_L = \infty$ .

## REFERENCES

- [1] M. F. Sultan, "Modeling of a bulk current injection setup for susceptibility threshold measurements," in *Proc. IEEE Int. Symp. Electromagn. Compat.*, San Diego, CA, 1986, pp. 188-195.
- [2] F. Grassi, S. A. Pignari, and F. Marliani, "Improved Lumped-Pi circuit model for bulk current injection probes," in *Proc. 2005 IEEE Int. Symp. Electromagn. Compat.*, Chicago, USA, Aug. 8-12, 2005, paper WE-AM-3-6.
- [3] Fischer Custom Communications Inc. Web-Site: <http://www.fischercc.com/>
- [4] A. E. Ruehli, "Inductance calculations in a complex integrated circuit environment," *IBM J. Research and Development*, vol. 16, pp. 470-481, 1972.